International Journal of ISSI, Vol. 12 (2015), No. 2, pp. 17-23

# Investigation of Wear Mechanism in Quenched and Tempered Medium Carbon-High Chromium Martensitic Steel Using Dry Sand/Rubber Wheel

S.M. Sehri [1], H. Ghayour [2*] , K. Amini [3], M. Naseri [4], H. Rastegari [5], V. Javaheri [6]

[1, 2] *Advanced Materials Research Center, Department of Materials Engineering, Najafabad Branch, Islamic Azad University , Najafabad, Isfahan , Iran*

[3] *Department of Mechanical Engineering, Tiran Branch, Islamic Azad University, Tiran, Isfahan, Iran*

[4, 6] *Research and Development, Isfahan Casting Industries Co., Isfahan, Iran*

[5] *Department of Mechanical and Materials Engineering, Birjand University of Technology, South Khorasan, Iran*

**Abstract**

The aim of the present study was to investigate the effect of quenching and tempering temperatures on the microstructure, mechanical properties and the wear characteristics of medium carbon-high chromium wear resistant steel. In addition, the dominant wear mechanisms were studied. For this purpose, austenitizing and tempering temperatures were selected in the ranges of 900-1000 °C and 300-500 °C, respectively. Mechanical properties were evaluated through hardness and impact tests as well as wear test (by dry sand/rubber wheel apparatus). Microstructure and wear and fracture surface appearances were investigated using scanning electron microscopy (SEM). Moreover, the measurement of retained austenite was done through X-Ray diffraction (XRD) analysis. The obtained results revealed that the best wear properties were achieved by tempering at 450 °C due to the reduction of tendency to micro-cracking, the decrease in internal stresses, and the improvement of the impact energy. Observing the wear surfaces showed that the wear mechanism for the specimen tempered at 400 °C was a combination of abrasive, adhesive and fatigue wear. However, abrasive wear was the only active wear mechanism for the specimen tempered at 450 °C.

*Keywords:* Medium carbon-high chromium wear resistant steel, Tempering, Dry sand/rubber-wheel abrasion, Wear mechanism.

## 1. Introduction

High chromium steels are widely used in mill linings due to high wear and impact resistance along with relatively low manufacturing costs. Severe wear or failure of the linings results in the loss of efficiency or even halt in mill operation and also, the rise of the cost of consumable parts. In this regard, proper application of heat treatment to obtain the desirable microstructure and get the required mechanical properties has an important influence on the performance of the different components [1-4]. Hardness, ductility, microstructure and chemical composition can be considered as the main metallurgical parameters affecting the wear behavior of different parts [5]. Since wear mechanisms include both plastic deformation and brittle fracture, it must be noted that hardness and toughness of the material have a major contribution in plastic deformation and brittle fracture, respectively [6]. Toughness is the most important parameter when micro-cracking mechanism is also active in addition to micro-plowing and micro-shearing mechanisms [7]. Critical force required for crack initiation in a material is decreased with increasing the hardness. Under such circumstances, brittle fracture and wear by micro-cracking mechanism are possible. Hence, under severe wear conditions in which a very hard material must be used, fracture toughness is a major determining factor in selecting the suitable material. High fracture toughness causes a decrease in the critical force required for cracking, thereby reducing the possibility of the brittle fracture and the activation of micro-cracking mechanism [8]. By increasing the toughness up to a certain value, the abrasive wear resistance is improved. However, exceeding this certain value leads to the reduction of wear resistance andas a consequence, wear becomes dependent on the hardness of the material [9]. Previous

* *Corresponding author*
*Email: ghayour_ham@iust.ac.ir*
*Address: Advanced Materials Research Center , Department of Materials Engineering, Najafabad Branch , Islamic Azad University , Najafabad , Isfahan , Iran*
*1. M.Sc. Student*
*2. Assisant Professor*
*3. Associate Professor*
*4. M.Sc.*
*5. Assistant Professor*
*6. M.Sc.*

studies have shown that the presence of hard particles such as complex carbides in the tempered martensite matrix can have a significant effect on the enhancement of the wear resistance by preventing the formation of abrasive grooves [10-12]. Jiang et al. [13] observed that for Fe-0.6C-1.5Cr-0.4Mo wear resistant steels, increasing the temperature of tempering process resulted in the precipitation of very fine ε carbides from martensite and bainite structures. Reduction of the carbon content in martensite structure increased its toughness and consequently, enhanced the wear properties.

Albert et al. [14] investigated the wear behavior of different cast steels used in the mining industry. The results indicated that better mechanical properties, particularly hardness, were the main metallurgical factor controlling the wear, especially when abrasive wear was dominant. Investigations conducted by Amini et al. [15] on the DIN 1.4057 steel revealed that secondary hardening phenomenon was activated by tempering in the temperature range of 350-450°C, resulting in the precipitation of the $M_7C_3$ carbides and the reduction of the amount of the retained austenite. In addition, drastic drop in hardness at 450-650 °C could be attributed to the transformation of the $M_7C_3$ carbides to $M_{23}C_6$ and also, microstructure coarsening. Naseri et al. [16] studied the AISI 420 martensitic stainless steel and reported that secondary hardening phenomenon at 400-500 °C was related to the precipitation of the $M_7C_3$ carbides.

This research was carried out on a commercial steel making company with the brand FMU29 Megato, Germany. There has been no analysis of this steel in any standard. Therefore, there is no information regarding the heat treatment of steel and also, the type of behavior in wear conditions. The innovative part of this article has been determining the optimum cycle for heat treatment of steel, surveying wear mechanism, and improving wear properties. Dry sand/rubber wheel method was used in order to adequately reproduce the wear conditions in the milling process.

## 2. Experimental Procedure

The considered alloy was prepared by melting high chromium steel scrapes and rejected castings along with ferroalloys using an electric induction furnace. Chemical composition of the obtained medium carbon-high chromium wear resistant steel was determined by Foundry-Master quantometer, as shown in Table 1.

The prepared specimen was heat treated under a vacuum of $5\times10^{-4}$ bar. For conventional heat treatment, at first, the specimens were austenitized at 900, 950 and 1000 °C for 15 minutes. After quenching in oil, they were tempered in the temperature range of 300- 500 °C with 50 °C intervals (Table 2).

*Table 1. Chemical composition of medium carbon-high chromium steel.*

| Element (%) | C | Si | Mn | P | S | Cr | Mo | Ni |
|---|---|---|---|---|---|---|---|---|
| Composition (wt. %) | 0.35 | 0.5 | 0.8 | <0.009 | <0.005 | 6.3 | 0.07 | 0.15 |

*Table 2. The heat treatment conditions of specimens.*

| Sample | Temperature austenitized (°C) | Time austenitized (min) | Quenching | Temperature tempered ( °C) | Time tempered (min) |
|---|---|---|---|---|---|
| A2 | 900 | 15 | oil | - | - |
| A2 | 950 | 15 | oil | - | - |
| A3 | 1000 | 15 | oil | - | - |
| T1 | 950 | 15 | oil | 300 | 60 |
| T2 | 950 | 15 | oil | 350 | 60 |
| T3 | 950 | 15 | oil | 400 | 60 |
| T4 | 950 | 15 | oil | 450 | 60 |
| T5 | 950 | 15 | oil | 500 | 60 |

X-Ray diffraction (XRD) analysis was performed in accordance with the ASTM E975-00 standard, using a Philips PW3040 diffractometer with Cukα radiation (1.5405 $\AA$ wavelength). The amount of the retained austenite in the microstructure can be calculated by equation (1), where Vγ is the austenite volume percentage and Iγ and Iα are the XRD intensities corresponding to the $(111)_\gamma$ and $(110)_\alpha$ planes, respectively [17].

$$V_\gamma = \frac{1.4I_\gamma}{I_a + 1.4I_\gamma} \qquad \text{Eq. (1)}$$

For microstructural observations and wear investigations, Olympus PME3 optical microscope and Philips XL30 scanning electron microscope (SEM) were used. Vilella's reagent (1 g picric acid, 10 ml hydrochloric acid and 100 ml ethanol) was employed to reveal the specimens microstructure. Rockwell C hardness measurements were done according to the ASTM E18 standard, using a Koopa-UV1 digital hardness tester. For each specimen, the hardness value was obtained from at least five points and the average value was reported. Room temperature Charpy impact tests were performed on the heat treated specimens with the dimensions of 55×10×10 mm based on the ASTM E23-2a standard, using a Pars Paygar impact testing machine with a capacity up to 160 J. For each heat treatment cycle, 6 impact test specimens were tested and the average impact energy was reported.

Wear test was conducted according to the ASTM G65-00 standard, using a dry sand abrasive wheel. Wear test specimens with the dimensions of 76×25×10 mm were cut from Y-blocks and subjected to heat treatment. Fig. 1 shows the dry sand/rubber abrasive wheel apparatus [18].

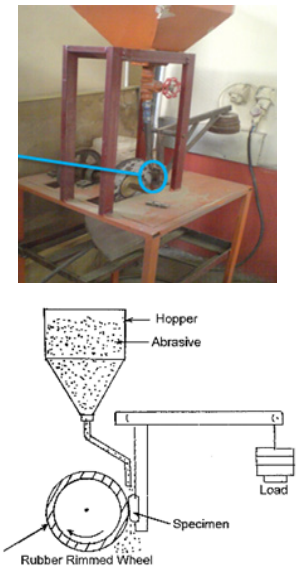


*Fig. 1. The dry sand/ rubber wheel apparatus [18].*

In this test, the rubber wheel rotated at a constant speed of 200 rpm and by applying a certain load on the contact location of specimen with the wheel (depending on the type of the selected method), a vertical force of 130 N was exerted. The abrasive material was $SiO_2$ sand (quartz) with the particle size of 212-300 μm. The moisture content of the sand had to be less than 5 %. In this apparatus, the abrasive was fed via a jet known as the sand jet, with a uniform feeding rate of 350 gr/min between the specimen and the rotating rubber wheel [18].

## 3. Results and discussion

Fig. 2 demonstrates the microstructure of the specimens austenitized at different temperatures. It was clear that the austenite grain size was relatively increased by raising the austenitizing temperature. This was due to the dissolution of the alloying carbides at higher temperatures acting as barriers to the growth of austenite grains. By the elimination of these carbides through dissolution in the matrix, austenite grain coarsening could occur more easily [15]. By using the Image J software, the grain size measured for specimens A1, A2, and A3 was calculated to be 61, 72, and 96 micron, respectively.

Variation of hardness has been plotted against the austenitizing temperature in Fig. 3. At the lowest austenitizing temperature, i.e. 900 °C (A1), carbon and chromium concentrations were very low in the austenite phase due to the little dissolution of carbides in the austenite matrix under low temperatures; therefore, the martensite obtained by quenching this C/Cr depleted austenite had a low hardness value. By increasing the austenitizing temperature up to 950 °C (A2), larger amounts of carbon and chromium were dissolved in the austenite phase and the degree of tetragonality was increased as a result of high stresses in the lattice [19]. Consequently, higher hardness and volume fraction of martensite were achieved. At 1000 °C (A3), because of the dissolution of large amounts of carbides in the austenite matrix and hence, the reduction of the retained carbides, excessive austenite grain growth occurred. On the other hand, the high concentration of the alloying elements in austenite decreased the Ms and $M_f$ temperatures, resulting in a larger amount of the retained austenite after quenching. Therefore, a softer martensite could be formed in this situation [20, 21]. Hsu et al. [22] stated that the reason for the reduction of transformation temperature by increasing the austenitinzing temperature was the joining of vacancy clusters to dislocations. As a result, martensite nucleation was retarded.

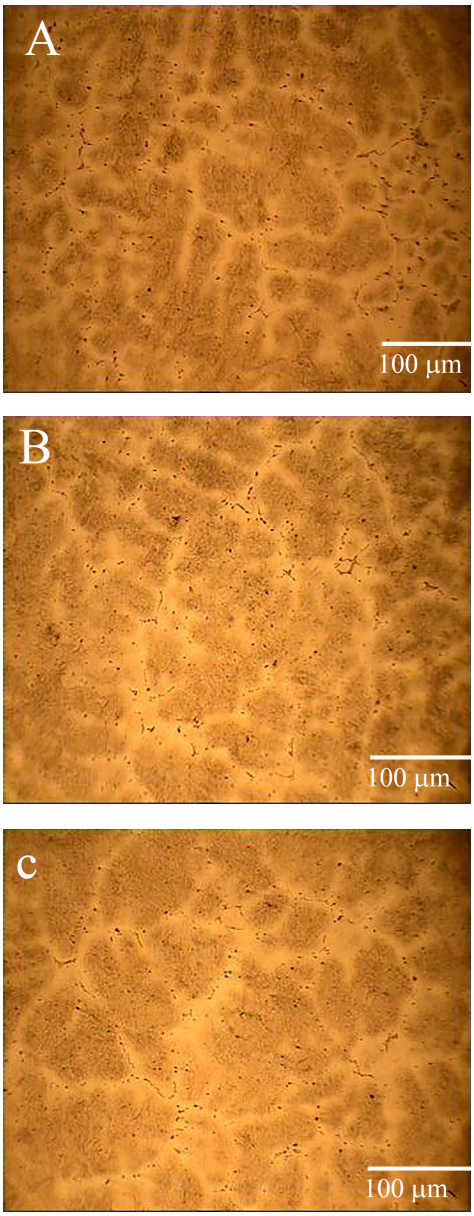


*Fig. 2. Microstructure of the austenitized specimens A) A1, B) A2, and C) A3.*

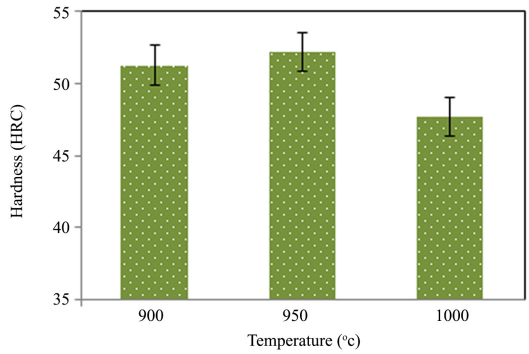


*Fig. 3. Variation of hardness with austenitizing temperature for 15 min.*

Fig. 4 shows the SEM micrographs of the microstructure of T3 and T4 specimens. Distribution of the carbides in martensite matrix could be clearly seen in the micrographs. According to this figure, in specimen T3 (Fig. 4 A), fine carbides were uniformly distributed in the matrix;this was the main reason for the higher hardness and better wear properties of the specimens tempered at this temperature, as compared to those tempered at lower temperatures. By increasing the tempering temperature to that of the specimen T4 (Fig. 4 B), the amount of the precipitated carbides was decreased and larger carbides were formed throughout the matrix. A martensite matrix with a uniform distribution of secondary carbides is necessary for achieving the desired properties. The matrix phase also contributes to the strong adherence of the carbides to the matrix and supports them against wear [19].

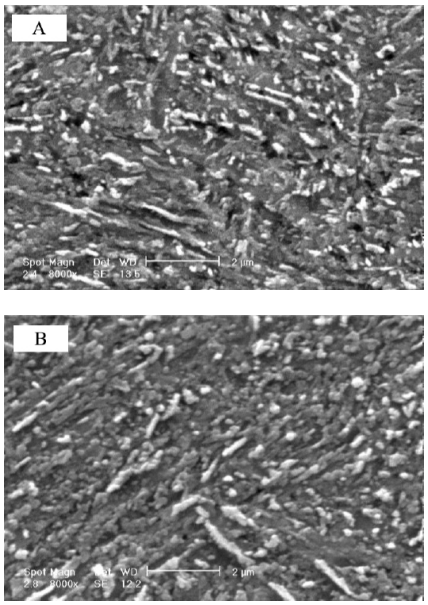


*Fig. 4. SEM micrographs of precipitated carbides dispersed in the specimens (A) T3 and (B) T4.*

Fig. 5 shows the variation of hardness as a function of the tempering temperature. As can be seen, by raising the tempering temperature from specimen T1 to specimen T3, hardness was increased due to secondary hardening phenomenon occurring because of the transformation of the retained austenite to martensite and the precipitation of the $M_7C_3$ carbide [16, 23]. The reasons for the increase in hardness value could be the high hardness of the carbide, strong embedding of carbide particles in the martensite matrix and the transformation of the retained austenite to martensite [19, 24]. By tempering in the temperature range of 400-500 °C (T3-T5), hardness was decreased, probably due to the transformation of a significant volume fraction of un-tempered martensite, the transformation of the $M_7C_3$ carbides to the $M_{23}C_6$ carbides and also,

carbide particle coarsening [16, 23- 24].

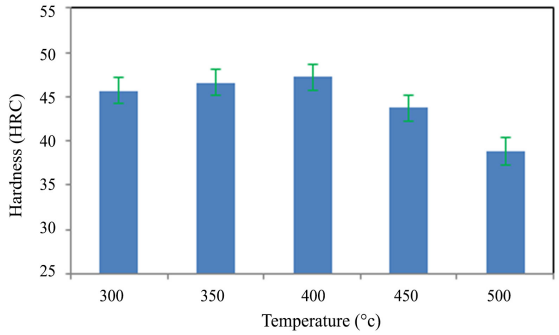


*Fig. 5. Variation of hardness with the tempering temperature.*

The XRD patterns for the quenched and quenched-tempered specimens are shown in Fig. 6. Quantitative studies indicated the presence of about 12% and less than 5% retained austenite in the quenched and quenched-tempered specimens, respectively. It could be clearly observed from Fig. 6 that the intensity of austenite peaks was reduced after the tempering process. These results confirmed the high values of hardness measured for the specimen T3.

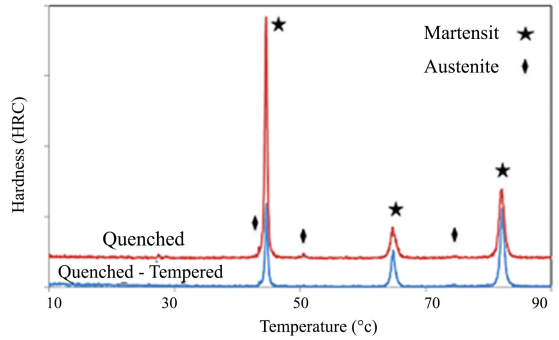


*Fig. 6. The XRD patterns for the quenched and quenched-tempered specimens.*

Fig. 7 demonstrates the effect of tempering temperature on the impact energy of the heat treated specimens. As can be observed, the impact energy was decreased by increasing the tempering temperature up to the specimen T3. Further increasing this temperature up to the specimen T5 resulted in an increase in the impact energy [16].

Changes in hardness and impact energy could be attributed to the precipitation of carbides during tempering. Hence, reduction of the impact energy by the specimen T3 could be explained by the formation of the $M_7C_3$ carbides and the decrease in the amount of the retained austenite, causing an increase in the hardness value. In addition, the impact energy was increased by tempering above 450 °C as a result of the transformation of a substantial fraction of martensite to tempered martensite, which was followed by the transformation of the tempered martensite to ferrite and cementite [15].

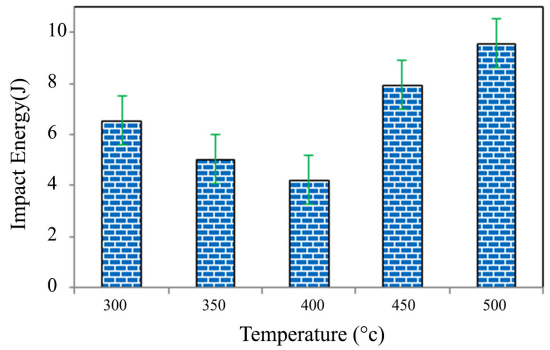


*Fig. 7. Variation of impact energy with the tempering temperature.*

The fracture surfaces of impact tested specimens T3 and T4 are presented in Fig. 8. No significant difference was observed between these fracture surfaces. Given that the impact energy of both specimens was relatively equal, this result was already expected. As can be seen in Fig. 8, cleavage fracture occurred, indicating the brittle fracture.

Wear tests were performed using dry sand/rubber wheel. Fig. 9 shows the amount of weight loss after 30 minutes for specimens tempered at different temperatures. By increasing the tempering temperature from the specimen T3 to the specimen T4, wear properties were improved and weight loss was reduced. However, weight loss began to increase again for the specimen T5.

In the tempering temperature range of the specimen T1 to the specimen T5, wear properties were enhanced because of the higher hardness of the specimens. At specimen T4, although a lower hardness value was obtained, better wear properties were observed due to the reduction of internal stresses, the higher ductility of the matrix, the higher impact energy and consequently, the lower tendency to micro-cracking. By the specimen T5, despite achieving higher ductility and impact energy in the matrix, wear properties were declined, mainly owing to the drastic decrease in hardness. Gupta et al. [25] found that by increasing the toughness up to a certain extent, abrasive wear resistance was improved. Nonetheless, if toughness exceeded this certain value, wear resistance would be reduced, because of thedependence on the hardness value. Hanguang and coworkers [26] studied the Fe-0.6C-1.5Cr low alloy Cr-Mo wear resistant steel and showed that wear resistance was strongly affected by hardness and toughness. They also reported that at 350 °C, optimum compromise between hardness and toughness was achieved, resulting in improved wear resistance. These results were in agreement with those obtained by Jiang et al. [27] for the Fe-0.75C-1Cr-0.8Mo wear resistant steel.

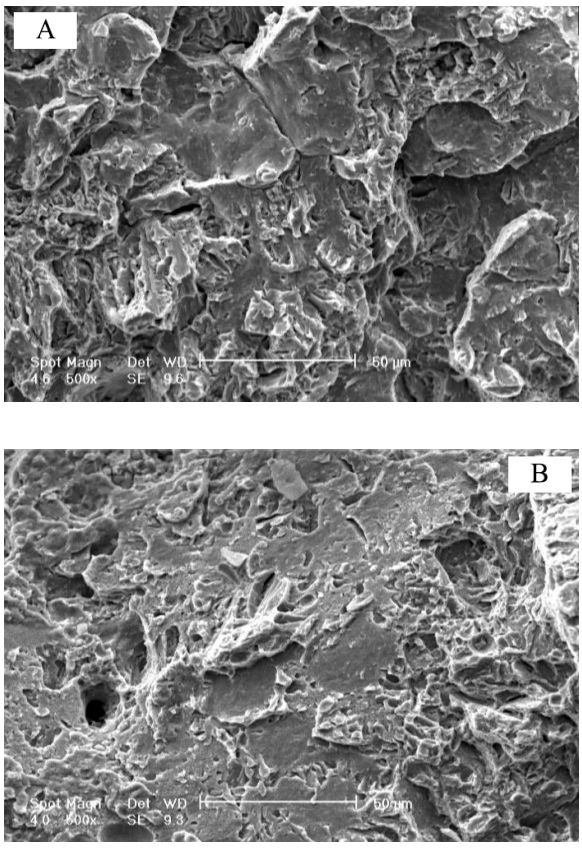


*Fig. 8. Fracture surfaces of specimens (A) T3 and (B) T4.*

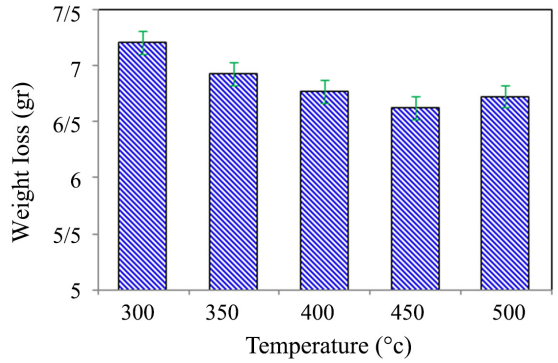


*Fig. 9. Weight loss versus tempering temperature.*

Surface appearance of the specimens was investigated using scanning electron microscopy to determine the wear mechanism. The wear surfaces of the specimens T3 and T4 are shown in Fig. 10. In both figures, typical grooves and ridges were observed on the abraded surfaces. Parallel grooves on both surfaces indicated micro-shearing abrasive wear mechanism [28, 29]. Accumulated particles on the surfaces werea product of wear and implied the domination of the adhesive wear mechanism [30-32]. By increasing the tempering temperature from the specimen T3 to the specimen T4, the width and depth of the grooves were reduced owing to the lower hardness and the higher toughness of the matrix in the latter situation. In addition, surface spalling became less significant by raising the tempering temperature. The specimen T3 was cut perpendicular to the wear passes for the further study of some local pits and ridges observed on its surface.

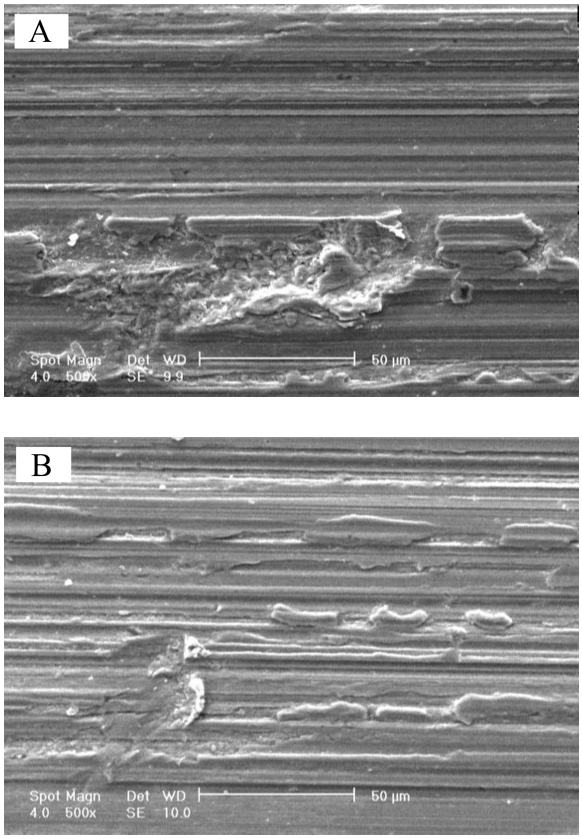


*Fig. 10. SEM images obtained from the specimens (A) T3 and (B) T4.*

SEM images of the surface perpendicular to the wear direction of the specimens quenched and tempered as T3 and T4 are presented in Fig. 11. For the specimen tempered at 400 °C, a series of spalling and fine cracks were observed, in addition to unevenness that resulted from micro-shearing. These spalling and cracks were a direct result of micro-cracking and fatigue mechanism (Fig. 11A) that occurred due to the reduction of the critical force required for crack formation because of the lower impact energy achieved by tempering at this temperature [32]. By increasing the tempering temperature to specimens T4, only the ridges typical of micro-shearing could be seen and micro-cracking and fatigue mechanism were hindered due to the reduction of hardness and the increase in ductility. Therefore, better wear properties were expected for the specimen T4, as compared to the one tempered at the specimen T3 (Fig. 11B).

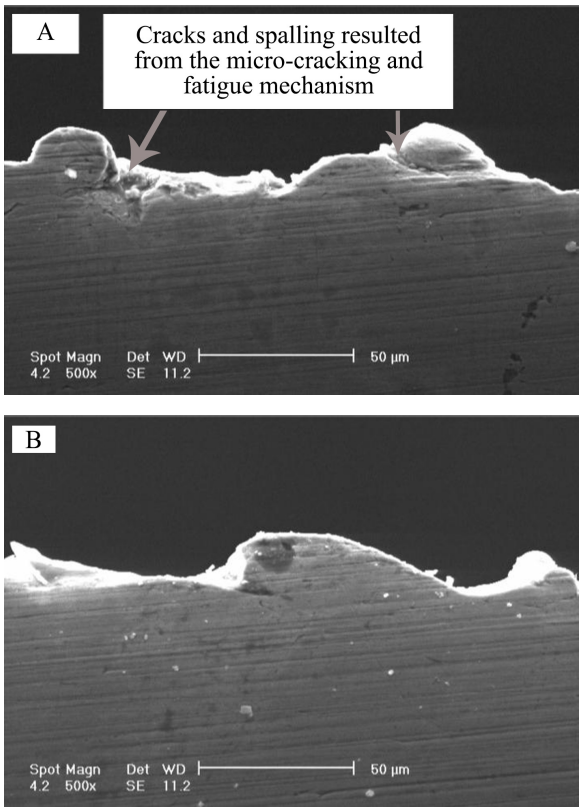


*Fig. 11. SEM images of the cross section of the specimens quenched and tempered (A) T3 and (B) T4.*

## 4. Conclusions

Secondary hardening phenomenon occurred during tempering in the temperature range of 300- 400 °C due to the transformation of the retained austenite to martensite, leading to a significant decrease in the impact energy.

- By tempering at 450 °C, wear properties were improved through the deactivation of micro-cracking and fatigue wear mechanism because of the lower hardness and the higher toughness of the matrix.
- For specimens tempered at 400 °C, wear mechanism included adhesive wear, fatigue, abrasive micro-shearing and abrasive micro-cracking. For the specimen tempered at 450 °C, only adhesive wear and micro-shearing could be recognized.
- Tempering at temperatures above 450 °C resulted in a drastic reduction of hardness and relative increase in the impact energy.
- During the tempering process, fine carbides were precipitated with uniform distribution, resulting in the improvement of wear properties.

## References

[1] P.W. Cleary: Minerals Eng., 14(2001), 1295.
[2] S. Banisi, M. Hadizadeh: Minerals Eng., 20(2007), 132.
[3] ASM Handbook, Heat Treating, Vol. 4, Third Edition, Metal Park, (1995).
[4] G. W. Stachowiak, A. Batchelor, Engineering Tribology, (2000).
[5] H. J. Yu, S. D. Bhole: Tribology. Int., 23(1990), 309.
[6] G. W. Stachowiak, A. Batchelor, Engineering Tribology, (2000).
[7] C. S. Ramesh, S. K. Seshadri, K. J. Lyer: Indian. J. Tech., 29(1991), 179.
[8] K. H. ZumGahr, Microstructure and Wear of Materials, Tribology Series, Institute of Materials Technology, Germany, (1987).
[9] A. K. Gupta, D. M. Jesudas, P. K. Das, K. Basu: Bio system. Eng., 88(2004), 63.
[10] L. Fang, Q. D. Zhou, Y. J. Li: Wear, 151(1991), 313.
[11] M. Dollar, I. M. Bernstain, A. W. Thompson: Act. Metal., 36(1988), 311.
[12] P. T. Mutton, J. D. Watson: Wear. 48(1978), 385.
[13] Z. Q. Jiang, J. M. Du, and X. L. FENG: J. iron steel research. Int., 13(2006), 57.
[14] D. L. Albright and D. J. Dunn: JOM. (1990), 23.
[15] K. Amini, M. R. Hoda, A. Shafyei: J. Metal Sci. and Heat, 55(2014), 499.
[16] A. Nasery Isfahany, H. Saghafian, Gh. Borhani: J. Alloys. Comp., 509(2011), 3931.
[17] J. Y. Huang, Y. T. Zhu: Mate Sci. Eng. A., 339(2003), 241.
[18] Standard Test Method for Measuring Abrasion Using the Dry Sand/Rubber Wheel Apparatus, ASTM International G 65–00a, (2000).
[19] G. Krauss, Steels Heat Treatment and Processing Principles, American Society for Metals, (1990).
[20] Chen Zhu, Tempering of Engineering Steels, Oxford Materials, (2005).
[21] R. C. Thomson, M. K. Miller: Act. Mat., 46(1998), 2203.
[22] T. Y. Hsu, Y. Linfah: Material Sci., 18(1983), 3213.
[23] R. C. Thomson, M. K. Miller: Act. Mat., 46(1998), 2203.
[24] K. P. Balan, A. Venugopal Reddy, and D. S. Sarma: J. Mater. Per., 8(1999), 385.
[25] A. K. Gupta, D. M. Jesudas, P. K. Das, K. Basu: Bio. Eng., 88(2004), 63.
[26] F. Hanguang, X. Qiang, F. Hanfeng: Mate. Sci. Eng. A., 396(2005), 206.
[27] Z. Q. Jiang, J. M. Du, and X. L. FENG: J. iron steel research. Int., 13(2006), 57.
[28] L. Bourithisa, G.D. Papadimitrioua, J. Sideris: Tribology Int., 39(2006), 479.
[29] A.K. Jha, B.K. Prasad, O.P. Modi, S. Das, A.H. Yegneswaran: Wear, 254(2003), 120.
[30] J. Yang, Y. Liu, Z. Ye, D. Yang, S. He: Surf. Coat. Technology, 204(2009), 705.
[31] F. Velasco, M. A. Martinez, R. Calabres, A. Bautista and J. Abenojar: Tribology Int., 42(2009), 1192.
[32] A. Ben CheikhLarbi, A. Cherif and M. A. Tarres: Wear, 258(2005), 712.